

Pseudorapidity asymmetry and centrality dependence of charged hadron spectra in $d+Au$ collisions at $\sqrt{s_{NN}}=200$ GeV

J. Adams,³ M. M. Aggarwal,²⁹ Z. Ahammed,⁴³ J. Amonett,²⁰ B. D. Anderson,²⁰ D. Arkhipkin,¹³ G. S. Averichev,¹² Y. Bai,²⁷ J. Balewski,¹⁷ O. Barannikova,³² L. S. Barnby,³ J. Baudot,¹⁸ S. Bekele,²⁸ V. V. Belaga,¹² R. Bellwied,⁴⁶ J. Berger,¹⁴ B. I. Bezverkhny,⁴⁸ S. Bharadwaj,³³ A. Bhasin,¹⁹ A. K. Bhati,²⁹ V. S. Bhatia,²⁹ H. Bichsel,⁴⁵ A. Billmeier,⁴⁶ L. C. Bland,⁴ C. O. Blyth,³ B. E. Bonner,³⁴ M. Botje,²⁷ A. Boucham,³⁸ A. V. Brandin,²⁵ A. Bravar,⁴ M. Bystersky,¹¹ R. V. Cadman,¹ X. Z. Cai,³⁷ H. Caines,⁴⁸ M. Calderón de la Barca Sánchez,¹⁷ J. Castillo,²¹ D. Cebra,⁷ Z. Chajecski,⁴⁴ P. Chaloupka,¹¹ S. Chattopdhyay,⁴³ H. F. Chen,³⁶ Y. Chen,⁸ J. Cheng,⁴¹ M. Cherney,¹⁰ A. Chikhanian,⁴⁸ W. Christie,⁴ J. P. Coffin,¹⁸ T. M. Cormier,⁴⁶ J. G. Cramer,⁴⁵ H. J. Crawford,⁶ D. Das,⁴³ S. Das,⁴³ M. M. de Moura,³⁵ A. A. Derevschikov,³¹ L. Didenko,⁴ T. Dietel,¹⁴ S. M. Dogra,¹⁹ W. J. Dong,⁸ X. Dong,³⁶ J. E. Draper,⁷ F. Du,⁴⁸ A. K. Dubey,¹⁵ V. B. Dunin,¹² J. C. Dunlop,⁴ M. R. Dutta Mazumdar,⁴³ V. Eckardt,²³ W. R. Edwards,²¹ L. G. Efimov,¹² V. Emelianov,²⁵ J. Engelage,⁶ G. Eppley,³⁴ B. Erazmus,³⁸ M. Estienne,³⁸ P. Fachini,⁴ J. Faivre,¹⁸ R. Fatemi,¹⁸ J. Fedorisin,¹² K. Filimonov,²¹ P. Filip,¹¹ E. Finch,⁴⁸ V. Fine,⁴ Y. Fisyak,⁴ K. Fomenko,¹² J. Fu,⁴¹ C. A. Gagliardi,³⁹ L. Gaillard,³ J. Gans,⁴⁸ M. S. Ganti,⁴³ L. Gaudichet,³⁸ F. Geurts,³⁴ V. Ghazikhanian,⁸ P. Ghosh,⁴³ J. E. Gonzalez,⁸ O. Grachov,⁴⁶ O. Grebenyuk,²⁷ D. Grosnick,⁴² S. M. Guertin,⁸ Y. Guo,⁴⁶ A. Gupta,¹⁹ T. D. Gutierrez,⁷ T. J. Hallman,⁴ A. Hamed,⁴⁶ D. Hardtke,²¹ J. W. Harris,⁴⁸ M. Heinz,² T. W. Henry,³⁹ S. Heppelmann,³⁰ B. Hippolyte,¹⁸ A. Hirsch,³² E. Hjort,²¹ G. W. Hoffmann,⁴⁰ H. Z. Huang,⁸ S. L. Huang,³⁶ E. W. Hughes,⁵ T. J. Humanic,²⁸ G. Igo,⁸ A. Ishihara,⁴⁰ P. Jacobs,²¹ W. W. Jacobs,¹⁷ M. Janik,⁴⁴ H. Jiang,⁸ P. G. Jones,⁵ E. G. Judd,⁶ S. Kabana,² K. Kang,⁴¹ M. Kaplan,⁹ D. Keane,²⁰ V. Yu. Khodyrev,³¹ J. Kiryluk,²² A. Kisiel,⁴⁴ E. M. Kislov,¹² J. Klay,²¹ S. R. Klein,²¹ D. D. Koetke,⁴² T. Kollegger,¹⁴ M. Kopytine,²⁰ L. Kotchenda,²⁵ M. Kramer,²⁶ P. Kravtsov,²⁵ V. I. Kravtsov,³¹ K. Krueger,¹ C. Kuhn,¹⁸ A. I. Kulikov,¹² A. Kumar,²⁹ R. Kh. Kutuev,¹³ A. A. Kuznetsov,¹² M. A. C. Lamont,⁴⁸ J. M. Landgraf,⁴ S. Lange,¹⁴ F. Laue,⁴ J. Lauret,⁴ A. Lebedev,⁴ R. Lednicky,¹² S. Lehocka,¹² M. J. LeVine,⁴ C. Li,³⁶ Q. Li,⁴⁶ Y. Li,⁴¹ G. Lin,⁴⁸ S. J. Lindenbaum,²⁶ M. A. Lisa,²⁸ F. Liu,⁴⁷ L. Liu,⁴⁷ Q. J. Liu,⁴⁵ Z. Liu,⁴⁷ T. Ljubicic,⁴ W. J. Llope,³⁴ H. Long,⁸ R. S. Longacre,⁴ M. Lopez-Noriega,²⁸ W. A. Love,⁴ Y. Lu,⁴⁷ T. Ludlam,⁴ D. Lynn,⁴ G. L. Ma,³⁷ J. G. Ma,⁸ Y. G. Ma,³⁷ D. Magestro,²⁸ S. Mahajan,¹⁹ D. P. Mahapatra,¹⁵ R. Majka,⁴⁸ L. K. Mangotra,¹⁹ R. Manweiler,⁴² S. Margetis,²⁰ C. Markert,²⁰ L. Martin,³⁸ J. N. Marx,²¹ H. S. Matis,²¹ Yu. A. Matulenko,³¹ C. J. McClain,¹ T. S. McShane,¹⁰ F. Meissner,²¹ Yu. Melnick,³¹ A. Meschanin,³¹ M. L. Miller,²² N. G. Minaev,³¹ C. Mironov,²⁰ A. Mischke,²⁷ D. K. Mishra,¹⁵ J. Mitchell,³⁴ B. Mohanty,⁴³ L. Molnar,³² C. F. Moore,⁴⁰ M. J. Mora-Corral,²³ D. A. Morozov,³¹ M. G. Munhoz,³⁵ B. K. Nandi,⁴³ S. K. Nayak,¹⁹ T. K. Nayak,⁴³ J. M. Nelson,³ P. K. Netrakanti,⁴³ V. A. Nikitin,¹³ L. V. Nogach,³¹ S. B. Nurushev,³¹ G. Odyniec,²¹ A. Ogawa,⁴ V. Okorokov,²⁵ M. Oldenburg,²¹ D. Olson,²¹ S. K. Pal,⁴³ Y. Panebratsev,¹² S. Y. Panitkin,⁴ A. I. Pavlinov,⁴⁶ T. Pawlak,⁴⁴ T. Peitzmann,²⁷ V. Perevoztchikov,⁴ C. Perkins,⁶ W. Peryt,⁴⁴ V. A. Petrov,¹³ S. C. Phatak,¹⁵ R. Picha,⁷ M. Planinic,⁴⁹ J. Pluta,⁴⁴ N. Porile,³² J. Porter,⁴⁵ A. M. Poskanzer,²¹ M. Potekhin,⁴ E. Potrebenikova,¹² B. V. K. S. Potukuchi,¹⁹ D. Prindle,⁴⁵ C. Pruneau,⁴⁶ J. Putschke,²³ G. Rakness,³⁰ R. Raniwala,³³ S. Raniwala,³³ O. Ravel,³⁸ R. L. Ray,⁴⁰ S. V. Razin,¹² D. Reichhold,³² J. G. Reid,⁴⁵ G. Renault,³⁸ F. Retiere,²¹ A. Ridiger,²⁵ H. G. Ritter,²¹ J. B. Roberts,³⁴ O. V. Rogachevskiy,¹² J. L. Romero,⁷ A. Rose,⁴⁶ C. Roy,³⁸ L. Ruan,³⁶ R. Sahoo,¹⁵ I. Sakrejda,²¹ S. Salur,⁴⁸ J. Sandweiss,⁴⁸ M. Sarsour,¹⁷ I. Savin,¹³ P. S. Sazhin,¹² J. Schambach,⁴⁰ R. P. Scharenberg,³² N. Schmitz,²³ K. Schweda,²¹ J. Seger,¹⁰ P. Seyboth,²³ E. Shahaliev,¹² M. Shao,³⁶ W. Shao,⁵ M. Sharma,²⁹ W. Q. Shen,³⁷ K. E. Shestermanov,³¹ S. S. Shimanskiy,¹² E. Sichtermann,²¹ F. Simon,²³ R. N. Singaraju,⁴³ G. Skoro,¹² N. Smirnov,⁴⁸ R. Snellings,²⁷ G. Sood,⁴² P. Sorensen,²¹ J. Sowinski,¹⁷ J. Speltz,¹⁸ H. M. Spinka,¹ B. Srivastava,³² A. Stadnik,¹² T. D. S. Stanislaus,⁴² R. Stock,¹⁴ A. Stolpovsky,⁴⁶ M. Strikhanov,²⁵ B. Stringfellow,³² A. A. P. Suaide,³⁵ E. Sugarbaker,²⁸ C. Suire,⁴ M. Sumbera,¹¹ B. Surrow,²² T. J. M. Symons,²¹ A. Szanto de Toledo,³⁵ P. Szarwas,⁴⁴ A. Tai,⁸ J. Takahashi,³⁵ A. H. Tang,²⁷ T. Tarnowsky,³² D. Thein,⁸ J. H. Thomas,²¹ S. Timoshenko,²⁵ M. Tokarev,¹² T. A. Trainor,⁴⁵ S. Trentalange,⁸ R. E. Tribble,³⁹ O. D. Tsai,⁸ J. Ulery,³² T. Ullrich,⁴ D. G. Underwood,¹ A. Urkinbaev,¹² G. Van Buren,⁴ M. van Leeuwen,²¹ A. M. Vander Molen,²⁴ R. Varma,¹⁶ I. M. Vasilevski,¹³ A. N. Vasiliev,³¹ R. Vernet,¹⁸ S. E. Vigdor,¹⁷ Y. P. Viyogi,⁴³ S. Vokal,¹² S. A. Voloshin,⁴⁶ M. Vznuzdaev,²⁵ W. T. Waggoner,¹⁰ F. Wang,³² G. Wang,²⁰ G. Wang,⁵ X. L. Wang,³⁶ Y. Wang,⁴⁰ Y. Wang,⁴¹ Z. M. Wang,³⁶ H. Ward,⁴⁰ J. W. Watson,²⁰ J. C. Webb,¹⁷ R. Wells,²⁸ G. D. Westfall,²⁴ A. Wetzler,²¹ C. Whitten, Jr.,⁸ H. Wieman,²¹ S. W. Wissink,¹⁷ R. Witt,² J. Wood,⁸ J. Wu,³⁶ N. Xu,²¹ Z. Xu,⁴ Z. Z. Xu,³⁶ E. Yamamoto,²¹ P. Yepes,³⁴ V. I. Yurevich,¹² Y. V. Zanevsky,¹² H. Zhang,⁴ W. M. Zhang,²⁰ Z. P. Zhang,³⁶ R. Zoukarneev,¹³ Y. Zoukarneeva,¹³ and A. N. Zubarev¹²

(STAR Collaboration)

¹Argonne National Laboratory, Argonne, Illinois 60439, USA²University of Bern, CH-3012 Bern, Switzerland³University of Birmingham, Birmingham, United Kingdom⁴Brookhaven National Laboratory, Upton, New York 11973, USA⁵California Institute of Technology, Pasadena, California 91125, USA⁶University of California, Berkeley, California 94720, USA⁷University of California, Davis, California 95616, USA⁸University of California, Los Angeles, California 90095, USA⁹Carnegie Mellon University, Pittsburgh, Pennsylvania 15213, USA

- ¹⁰*Creighton University, Omaha, Nebraska 68178, USA*
¹¹*Nuclear Physics Institute AS CR, 250 68 Řež/Prague, Czech Republic*
¹²*Laboratory for High Energy (JINR), Dubna, Russia*
¹³*Particle Physics Laboratory (JINR), Dubna, Russia*
¹⁴*University of Frankfurt, Frankfurt, Germany*
¹⁵*Institute of Physics, Bhubaneswar 751005, India*
¹⁶*Indian Institute of Technology, Mumbai, India*
¹⁷*Indiana University, Bloomington, Indiana 47408, USA*
¹⁸*Institut de Recherches Subatomiques, Strasbourg, France*
¹⁹*University of Jammu, Jammu 180001, India*
²⁰*Kent State University, Kent, Ohio 44242, USA*
²¹*Lawrence Berkeley National Laboratory, Berkeley, California 94720, USA*
²²*Massachusetts Institute of Technology, Cambridge, Massachusetts 02139-4307, USA*
²³*Max-Planck-Institut für Physik, Munich, Germany*
²⁴*Michigan State University, East Lansing, Michigan 48824, USA*
²⁵*Moscow Engineering Physics Institute, Moscow, Russia*
²⁶*City College of New York, New York, New York 10031, USA*
²⁷*NIKHEF, Amsterdam, The Netherlands*
²⁸*Ohio State University, Columbus, Ohio 43210, USA*
²⁹*Panjab University, Chandigarh 160014, India*
³⁰*Pennsylvania State University, University Park, Pennsylvania 16802, USA*
³¹*Institute of High Energy Physics, Protvino, Russia*
³²*Purdue University, West Lafayette, Indiana 47907, USA*
³³*University of Rajasthan, Jaipur 302004, India*
³⁴*Rice University, Houston, Texas 77251, USA*
³⁵*Universidade de Sao Paulo, Sao Paulo, Brazil*
³⁶*University of Science & Technology of China, Anhui 230027, China*
³⁷*Shanghai Institute of Applied Physics, Shanghai 201800, China*
³⁸*SUBATECH, Nantes, France*
³⁹*Texas A&M University, College Station, Texas 77843, USA*
⁴⁰*University of Texas, Austin, Texas 78712, USA*
⁴¹*Tsinghua University, Beijing 100084, China*
⁴²*Valparaiso University, Valparaiso, Indiana 46383, USA*
⁴³*Variable Energy Cyclotron Centre, Kolkata 700064, India*
⁴⁴*Warsaw University of Technology, Warsaw, Poland*
⁴⁵*University of Washington, Seattle, Washington 98195, USA*
⁴⁶*Wayne State University, Detroit, Michigan 48201, USA*
⁴⁷*Institute of Particle Physics, CCNU (HZNU), Wuhan 430079, China*
⁴⁸*Yale University, New Haven, Connecticut 06520, USA*
⁴⁹*University of Zagreb, Zagreb HR-10002, Croatia*
- (Received 17 August 2004; published 23 December 2004)

The pseudorapidity asymmetry and centrality dependence of charged hadron spectra in d +Au collisions at $\sqrt{s_{NN}}=200$ GeV are presented. The charged particle density at midrapidity, its pseudorapidity asymmetry, and centrality dependence are reasonably reproduced by a multiphase transport model, by HIJING, and by the latest calculations in a saturation model. Ratios of transverse momentum spectra between backward and forward pseudorapidity are above unity for p_T below 5 GeV/ c . The ratio of central to peripheral spectra in d +Au collisions shows enhancement at $2 < p_T < 6$ GeV/ c , with a larger effect at backward rapidity than forward rapidity. Our measurements are in qualitative agreement with gluon saturation and in contrast to calculations based on incoherent multiple partonic scatterings.

DOI: 10.1103/PhysRevC.70.064907

PACS number(s): 25.75.Dw

Soft and hard scattering processes have distinctive rapidity and centrality dependences in the context of particle production in $d(p)$ +Au collisions. Models based on the color glass condensate [1,2], HIJING [3], and multiphase transport (AMPT) [4] predict specific pseudorapidity (η) and central-

ity dependence of produced particle density which can be directly compared to experimental measurements. The Cronin effect [5]—the enhancement of particle yield at intermediate transverse momentum (p_T) with respect to binary collision scaling—has also been observed in d +Au collisions at

RHIC [6–10]. For partonic processes such as the dominant $g+g$ and $q+g$ scatterings, the particle rapidity distribution can be evaluated in a pQCD-inspired framework that depends on the parton distribution functions and the underlying dynamics. For example, calculations of the Cronin effect based on incoherent initial multiple partonic scatterings and independent fragmentation [3] predict a unique rapidity asymmetry of particle production in $d+Au$ collisions, where the backward-to-forward [negative rapidity (Au) to positive rapidity (d)] particle ratio is greater than unity at low p_T , goes below unity at intermediate p_T , and approaches unity again at high p_T . The amplitude of the theoretical backward-to-forward particle ratios depends on the nuclear shadowing [3]. Calculations of shadowing alone, based on Regge theory and hard diffraction [11], are fairly successful in describing the observed suppression of particle production at forward rapidity in $d+Au$ collisions [12]. The calculation in Ref. [12] considers the spatial dependence of the shadowing, leading to an impact parameter dependence that goes beyond the simple geometrical scaling. Calculations in a gluon saturation model [13] predict a backward-to-forward particle ratio that is opposite to the predictions based on incoherent multiple partonic scatterings. In this approach, the particle production is related to the high gluon density in the nucleus (nucleon). The asymmetry is greater than unity in the range of transverse momenta determined by the values of the saturation scale $Q_s(y)$ and the geometrical scale $Q_s^2(y)/Q_{s,\min}$, where $Q_{s,\min}$ is at the onset of the gluon saturation. Recently, the quark recombination model was used to explain the Cronin effect as a final-state effect [14], implying a backward-to-forward particle ratio markedly different from that of the QCD-inspired formulation in [3] and similar to the predictions by a saturation model [13]. In this approach, the enhancement of particle production at intermediate p_T is an extension from low p_T due to the thermal parton and shower parton recombination [14].

The suppression of high transverse momentum particles in central Au+Au collisions at RHIC can be described by both final-state and initial-state effects, such as jet quenching calculations that assume parton energy loss via gluon bremsstrahlung [15,16] or gluon saturation [17]. The measurement of particle production at midrapidity from $d+Au$ collisions at RHIC [6–9] favors the scenario that the suppression of high- p_T particles is primarily due to the final-state interactions, i.e., processes after the hard partonic scattering. The quantitative features of high- p_T particle production in Au+Au collisions can be described by models that incorporate a combination of physical effects such as the Cronin effect, nuclear shadowing [18], and parton energy loss [15,16]. The Cronin effect and shadowing can be investigated in $d(p)+Au$ collisions. The magnitude of these nuclear effects on particle production has a geometrical dependence due to the nuclear density distribution. The particle production in $d(p)+Au$ collisions at different rapidities also reflects the dynamics of nuclear and Bjorken- x dependence of these effects. Therefore, the centrality, pseudorapidity, and p_T dependence of particle production in $d(p)+Au$ collisions provides an essential baseline for understanding the underlying phenomena in Au+Au collisions.

We present inclusive p_T spectra of charged hadrons over an η range of -1 (Au-side) to $+1$ (d -side) in $d+Au$ collisions at $\sqrt{s_{NN}}=200$ GeV with several collision centrality selections. For these measurements, the STAR time-projection chamber (TPC) [19] provided tracking of charged hadrons. The minimum bias trigger was defined by requiring that at least one beam-rapidity neutron impinge on the zero degree calorimeter [20] in the Au beam direction. The measured minimum bias cross section amounts to $95\pm 3\%$ of the total $d+Au$ geometric cross section. Charged particle multiplicity within $-3.8 < \eta < -2.8$ was measured by the forward TPC [21] in the Au beam direction and served as the basis for our $d+Au$ centrality tagging scheme, as described in [6]. The $d+Au$ centrality definition consists of three event centrality classes: the 0–20, 20–40, and 40–100 percentiles of the total $d+Au$ cross section. A separate centrality tag, which requires that a single neutron impinge on the zero degree calorimeter in the deuteron beam direction (ZDC- d), was also used. Our analysis was restricted to events with a primary vertex within 50 cm of the center of the TPC along the beam direction. This yielded a data set of 9.5×10^6 minimum bias events. Only tracks (with at least 15 measured points) with a projected distance of closest approach to the event primary vertex of less than 3 cm were used in the analysis.

Acceptance and TPC tracking efficiency corrections in various pseudorapidity regions and centrality classes were obtained by embedding simulated data into a real data sample. In the region of $|\eta| < 0.5$, the tracking efficiency and acceptance above $p_T=2.0$ GeV/ c were observed to reach a plateau of about 90% for all centrality classes. Efficiency corrections using filtered HIJING [22]—HIJING events in a GEANT simulation of the detector—were also used; a maximum difference between HIJING and embedded data of about 3% was observed. Background due to weak decay products was accounted for using filtered HIJING. For the 0–20 % most central events, the contaminating signals are estimated at less than 18% for $p_T < 1.0$ GeV/ c , and for the 40–100 % most peripheral events this was observed to be less than 12%. The background exponentially decreases, and above $p_T=1.0$ GeV/ c , the background is approximately 4%, exhibiting no strong dependence on centrality or pseudorapidity. A net uncertainty of 6% in the analysis corrections was determined by adding the efficiency and background correction uncertainties in quadrature.

The transverse momentum spectra of primary charged hadrons for various pseudorapidity regions are shown in Fig. 1 for the 0–20 %, 20–40 %, 40–100 % centrality selections, and for minimum bias events. In the region of $0.2 < p_T < 2.0$ GeV/ c , the charged hadron spectra were fitted with a power-law function,

$$\frac{d^2N}{p_T dp_T d\eta} = \frac{A}{(1 + p_T/p_0)^n}. \quad (1)$$

The integrated charged hadron multiplicity per unit of pseudorapidity $dN/d\eta$ was obtained by summing up the measured yields in the covered momentum range and using the power-law function for extrapolation to $p_T=0$ GeV/ c . Figure 2 shows the pseudorapidity dependence of charged particle

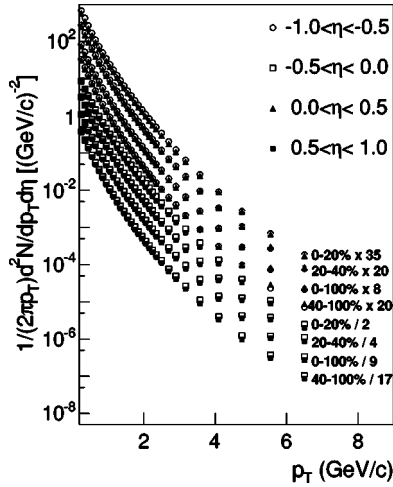


FIG. 1. The p_T spectra of charged hadrons. From the top, the open circles correspond to the 0–20 %, 20–40 %, minimum bias, and 40–100 % centralities in $-1.0 < \eta < -0.5$. Similarly, the solid triangles, open squares, and solid squares correspond to p_T spectra in $0.0 < \eta < 0.5$, $-0.5 < \eta < 0.0$, and $0.5 < \eta < 1.0$, respectively. Spectra have been scaled by the factors indicated in the figure.

densities for various centrality classes. Calculations based on the ideas of gluon saturation [1] in the color glass condensate as well as the predictions of AMPT [4] are also shown. Both models predict a similar pseudorapidity dependence of particle yields. It should be noted that the pseudorapidity and centrality dependence of charged particle yields generated by HIJING [22] (without shadowing) are nearly identical to the AMPT results at midrapidity. There is a clear increase in the asymmetry of charged particle densities as a function of increasing centrality: a prominent pseudorapidity dependence is observed for the 0–20 % most central collisions, while peripheral collisions between gold nuclei and deuterons are akin to symmetric $p+p$ collisions. The predictions of the

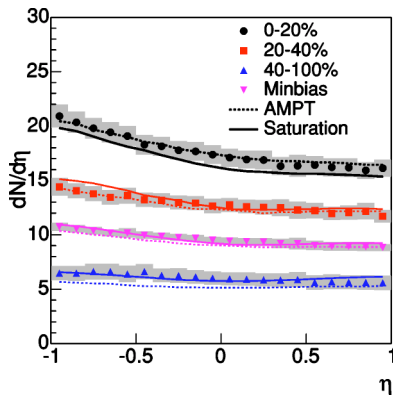


FIG. 2. (Color online) The pseudorapidity dependence of charged particle densities for various centrality classes. Particle tracking efficiency and background corrections were carried out for each pseudorapidity bin ($\Delta\eta=0.1$). The point-to-point systematic uncertainties shown for each distribution (indicated by bands) are the quadratic sum of the efficiency and background correction uncertainties; statistical uncertainties are negligible. The results of AMPT (with default parameters) and parton saturation are indicated by the dashed and solid lines, respectively.

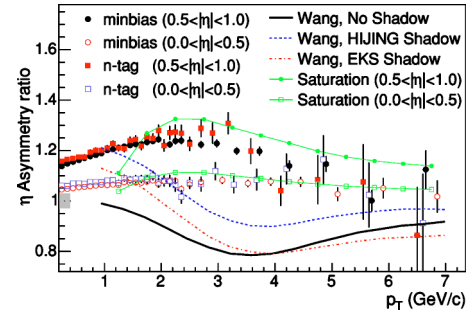


FIG. 3. (Color online) The ratio of charged hadron spectra in the backward rapidity to forward rapidity region for minimum bias and ZDC- d neutron-tagged events. Calculations based on pQCD [3] ($y=-1/y=1$) for minimum bias events are also shown for cases with no shadowing (solid curve), HIJING shadowing (dashed curve), and EKS shadowing (dot-dashed curve). Calculations in a gluon saturation model [13] for minimum bias events are shown for $0.5 < |\eta| < 1.0$ (filled circles with solid line) and for $0.0 < |\eta| < 0.5$ (open squares with solid line).

gluon saturation model and AMPT are in good overall agreement with the data.

We define a measured asymmetry by taking ratios of inclusive backward (Au-side) to forward (d -side) p_T spectra. Figure 3 shows the p_T dependence of the asymmetry for minimum bias and ZDC- d neutron-tagged events. The ratio was taken between the $-1.0 < \eta < -0.5$ and $0.5 < \eta < 1.0$ as well as $-0.5 < \eta < 0.0$ and $0.0 < \eta < 0.5$ regions. An overall systematic uncertainty (indicated by the band) of less than 3% was assessed by taking the corresponding ratios between inclusive spectra measured by STAR in $p+p$ collisions at the same energy, where an asymmetry is not expected to be present. The ratio taken within $|\eta| < 0.5$ is nearly constant in p_T , with a maximum value of approximately 1.075. This indicates that there is a small disparity between the forward and backward regions immediately around $\eta=0$. The ratio taken at higher pseudorapidity slowly increases with p_T up to about $p_T=2.5$ GeV/ c , attaining a value of approximately 1.25. The ratio taken at higher pseudorapidity approaches unity beyond $P_T=5$ GeV/ c , indicating the absence of nuclear effects at high p_T . For the ZDC- d neutron-tagged events, the ratio exhibits nearly the same p_T dependence as minimum bias events. Figure 4(a) illustrates the centrality dependence of the asymmetry in the region of $0.5 < |\eta| < 1.0$. The asymmetry becomes more prominent with increasing centrality, reaching a factor of about 1.35 for the most central events. The asymmetry in the region of $0.0 < |\eta| < 0.5$, shown in Fig. 4(b), does not exhibit a strong centrality and p_T dependence. The neutron-tagged events have an average number of binary collisions, $\langle N_{\text{bin}} \rangle = 2.9 \pm 0.2$, well below the $\langle N_{\text{bin}} \rangle = 7.5 \pm 0.4$ of the minimum bias data set. The events in which a single nucleon from the deuteron interacted with the Au nucleus comprise approximately half of the 40–100 % peripheral centrality class [6]. However, Fig. 3 shows that the η asymmetry ratios for minimum bias and neutron-tagged events are nearly identical.

Particle production at midrapidity in $d+Au$ collisions may include contributions from deuteron-side partons that have experienced multiple scatterings while traversing the gold

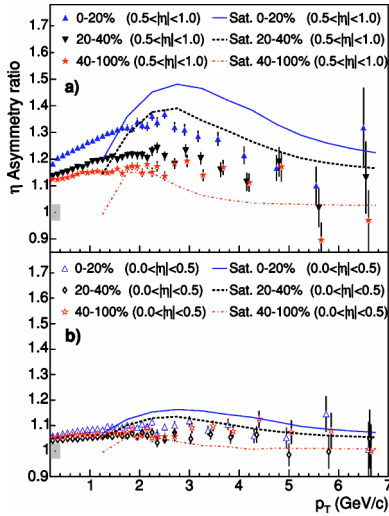


FIG. 4. (Color online) (a) The centrality dependence of the ratio of charged hadron spectra in backward rapidity to forward rapidity ($0.5 < |\eta| < 1.0$). The gluon saturation model calculations are also shown for the 0–20 % (solid curve), 20–40 % (dashed curve), and 40–100 % (dot-dashed curve) centrality classes. (b) The centrality dependence of the ratio of charged hadron spectra in backward rapidity to forward rapidity ($0.0 < |\eta| < 0.5$). The gluon saturation model calculations are also shown for the 0–20 % (solid curve), 20–40 % (dashed curve), and 40–100 % (dot-dashed curve) centrality classes.

nucleus, and from gold-side partons that may have been modified by nuclear effects. Also shown in Fig. 3 is the calculation of the asymmetry in the incoherent multiple partonic scattering framework with various nuclear shadowing parametrizations: no nuclear shadowing, the HIJING shadowing [23], and the EKS shadowing [24] parametrizations. The ratio, taken for minimum bias spectra at $y=-1$ and $y=1$, is below unity at $p_T \sim 3-4$ GeV/ c and is a consequence of the increase in p_T for partons from the deuteron hemisphere. Our measurements disagree with the theoretical calculations [3] and thus suggest that incoherent multiple scattering of partons in the initial state alone cannot reproduce the observed pseudorapidity asymmetry in the intermediate p_T region. By the same token, the class of models that incorporate initial parton scattering [3,4,25], though capable of reproducing integrated observables such as charged particle yield asymmetries, may not adequately reproduce the p_T dependence of the asymmetry. In this respect, the p_T dependence of the pseudorapidity asymmetry as illustrated by the backward-to-forward ratio of charged hadron spectra can serve as an important discriminator between models.

The minimum bias gluon saturation results for the backward-to-forward ratio of charged hadron spectra, also shown in Fig. 3, were obtained by performing a calculation identical to the one in Ref. [13] on the basis of the method developed in [17,26]. In this approach, the asymmetry is greater than unity in the range of transverse momenta determined by the values of the saturation scale $Q_s(y)$ and the geometrical scale $Q_s^2(y)/Q_{s,\min}$. The calculated particle yield asymmetry, evaluated over the same pseudorapidity range as the data, is in qualitative agreement with our observations.

The theoretical asymmetry exhibits a stronger p_T dependence than actually observed, overpredicting the magnitude of the asymmetry at high pseudorapidities. The centrality dependence of the backward-to-forward particle yields in a saturation model, illustrated in Fig. 4(a) and 4(b), qualitatively reproduces the observed centrality dependence. Although the model calculations fail to describe the data in detail, they show the same trend of increasing asymmetry with increasing centrality. We note that some conventional models [12,27] are able to reproduce the suppression of particle production at forward rapidity in $d+Au$ collisions, which was thought to be a unique feature of gluon saturation [2,13,28]. It will be interesting to quantitatively compare our measurements with those calculations in the future.

It should be noted that a strong particle dependence in the nuclear modification factor has been observed in this intermediate p_T region in both Au+Au [29] and $d+Au$ collisions [10]. Collective partonic effects at the hadron formation epoch such as parton coalescence or recombination [30–33] have been proposed to explain Au+Au results. The pseudorapidity asymmetry approaches unity at a p_T scale above 5 GeV/ c , approximately the same p_T scale above which the particle dependence of the nuclear modification factor disappears. The idea of recombination was modified to explain the Cronin effect and its particle dependence [14] as a final-state effect. In this approach, the enhancement of particle production at intermediate p_T is an extension from low p_T due to the thermal parton and shower parton recombination [14], qualitatively consistent with the measurements of the pseudorapidity asymmetry as a function of p_T . We should emphasize that the pseudorapidity asymmetry is not likely to be solely due to the change of particle composition. In the recombination model, the shower and thermal parton recombination not only enhances the baryon production, but also the meson production [14]. The pseudorapidity asymmetry of identified pion spectra and its quantitative comparison to models are important for further understanding of particle production at intermediate p_T .

Of similar interest is the ratio of $d+Au$ central to peripheral inclusive spectra

$$R_{CP}^{dAu} = \frac{(d^2N/dp_T d\eta \langle N_{\text{bin}} \rangle)_{\text{central}}}{(d^2N/dp_T d\eta \langle N_{\text{bin}} \rangle)_{\text{periph}}}, \quad (2)$$

where $d^2N/dp_T d\eta$ is the differential yield per event in collisions for a given centrality class and $\langle N_{\text{bin}} \rangle$ is the mean numbers of binary collisions corresponding to this centrality. Using a Monte Carlo Glauber calculation, as described in [6], the mean number of binary collisions for the 0–20 % and 40–100 % centrality classes was determined to be 15.0 ± 1.1 and 4.0 ± 0.3 , respectively. Figure 5 shows the ratio of the central to peripheral spectra in $d+Au$ collisions for various pseudorapidity regions. The error bars on each distribution are the quadratic sum of statistical and systematic uncertainties; the latter are due to uncertainties in our background subtraction technique. An overall error of about 10% due to the uncertainty in normalization is indicated by the band on the left portion of the figure. The R_{CP} in Au+Au collisions at $\sqrt{s_{NN}}=200$ GeV [34] is shown on the bottom of the plot. R_{CP}^{dAu}

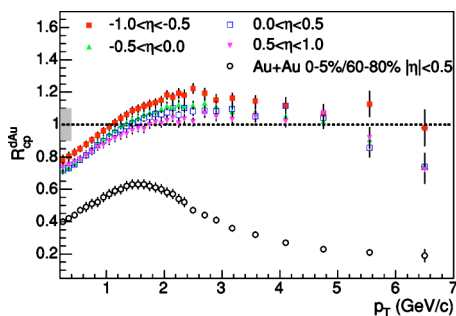


FIG. 5. (Color online) The ratio of central (0–20 %) to peripheral (40–100 %) spectra in $d+Au$ collisions for various pseudorapidity regions and in Au+Au collisions at midrapidity.

distributions for each pseudorapidity selection exhibit a rise with increasing p_T , exceeding unity at $p_T \sim 1-2$ GeV/ c . At low p_T , the R_{CP}^{dAu} distribution is highest for the most backward pseudorapidity region and systematically decreases the more forward in pseudorapidity the ratio is taken. The trend in the pseudorapidity dependence indicates that the Cronin effect is more pronounced in the gold hemisphere of the collision, consistent with the measured asymmetry between backward and forward rapidity. Our measurement of R_{CP}^{dAu} shows no significant suppression at p_T of 2–6 GeV/ c . This result stands in contrast to the Au+Au measurements, where R_{CP} was observed to be well below unity for $p_T < 12$ GeV/ c . The results for R_{CP}^{dAu} are consistent with calculations in pQCD models incorporating both Cronin enhancement and nuclear shadowing [25,35–38]. However, the models based on incoherent parton scattering at the initial stage fail to reproduce the rapidity dependence in both backward-to-forward ratios and R_{CP}^{dAu} .

In summary, we have studied the centrality and pseudorapidity dependence of charged hadron production in $d+Au$ collisions at $\sqrt{s_{NN}}=200$ GeV. The inclusive charged hadron multiplicity is observed to be higher in the gold hemisphere than the deuteron hemisphere of the collision. The gluon saturation, HIJING, and AMPT models cannot be ruled out from the integrated charged particle pseudorapidity distributions. Ratios of backward-to-forward pseudorapidity transverse momentum distributions are above unity for p_T below 5 GeV/ c . Our measurement of R_{CP}^{dAu} shows no suppression at p_T of 2–6 GeV/ c , with the ratio taken at backward pseudorapidities being slightly higher than at forward pseudorapidities. The incoherent multiple scattering of partons in the initial state alone cannot reproduce the observed pseudorapidity asymmetry, while the latest calculations in a gluon saturation model stand in qualitative agreement with our observations.

We are grateful to D. Kharzeev and K. Tuchin for providing us with their saturation results and X.N. Wang for valuable discussions and for providing us with the multiple partonic scattering results. We thank the RHIC Operations Group and RCF at BNL, and the NERSC Center at LBNL for their support. This work was supported in part by the HENP Divisions of the Office of Science of the U.S. DOE; the U.S. NSF; the BMBF of Germany; IN2P3, RA, RPL, and EMN of France; EPSRC of the United Kingdom; FAPESP of Brazil; the Russian Ministry of Science and Technology; the Ministry of Education and the NNSFC of China; Grant Agency of the Czech Republic, FOM and UU of the Netherlands, DAE, DST, and CSIR of the Government of India; Swiss NSF; and the Polish State Committee for Scientific Research.

-
- [1] D. Kharzeev, Nucl. Phys. **A730**, 448 (2004).
 [2] D. Kharzeev *et al.*, Phys. Lett. B **561**, 93 (2003); J. Jalilian-Marian *et al.*, *ibid.* **577**, 54 (2003); J.L. Albacete *et al.*, Phys. Rev. Lett. **92**, 082001 (2004); D. Kharzeev *et al.*, Phys. Rev. D **68**, 094013 (2003); R. Baier *et al.*, *ibid.* **68**, 054009 (2003).
 [3] X.N. Wang, Phys. Lett. B **565**, 116 (2003).
 [4] Z.W. Lin and C.M. Ko, Phys. Rev. C **68**, 054904 (2003).
 [5] J.W. Cronin *et al.*, Phys. Rev. D **11**, 3105 (1975).
 [6] J. Adams *et al.*, Phys. Rev. Lett. **91**, 072304 (2003).
 [7] S.S. Adler *et al.*, Phys. Rev. Lett. **91**, 072303 (2003).
 [8] B.B. Back *et al.*, Phys. Rev. Lett. **91**, 072302 (2003).
 [9] I. Arsene *et al.*, Phys. Rev. Lett. **91**, 072305 (2003).
 [10] J. Adams *et al.*, nucl-ex/0309012.
 [11] L. Frankfurt, V. Guzey, and M. Strikman, hep-ph/0303022.
 [12] R. Vogt, hep-ph/0405060.
 [13] D. Kharzeev, Y.V. Kovchegov, and K. Tuchin, hep-ph/0405045; D. Kharzeev and K. Tuchin (private communication).
 [14] R.C. Hwa and C.B. Yang, Phys. Rev. Lett. **93**, 082302 (2004); Phys. Rev. C **70**, 037901 (2004); R.C. Hwa (private communication).
 [15] M. Gyulassy and M. Plumer, Phys. Lett. B **243**, 432 (1990).
 [16] X.N. Wang and M. Gyulassy, Phys. Rev. Lett. **68**, 1480 (1992).
 [17] D. Kharzeev, E. Levin, and L. McLerran, Phys. Lett. B **561**, 93 (2003).
 [18] K.J. Eskola and H. Honkanen, Nucl. Phys. **A713**, 167 (2003).
 [19] M. Anderson *et al.*, Nucl. Instrum. Methods Phys. Res. A **499**, 659 (2003).
 [20] C. Adler *et al.*, Nucl. Instrum. Methods Phys. Res. A **461**, 337 (2001).
 [21] K.H. Ackermann *et al.*, Nucl. Instrum. Methods Phys. Res. A **499**, 713 (2003).
 [22] X.N. Wang and M. Gyulassy, Phys. Rev. D **44**, 3501 (1991). Version 1.382 is used.
 [23] S.Y. Li and X.N. Wang, Phys. Lett. B **527**, 85 (2002).
 [24] K.J. Eskola, V.J. Kolhinen, and C.A. Salgado, Eur. Phys. J. C **9**, 61 (1999).
 [25] A. Accardi, hep-ph/0212148, and references therein.
 [26] D. Kharzeev, Y.V. Kovchegov, and K. Tuchin, Phys. Rev. D **68**, 094013 (2003).
 [27] J. Qiu and I. Vitev, hep-ph/0405068.
 [28] I. Arsene *et al.*, nucl-ex/0403005.
 [29] J. Adams *et al.*, Phys. Rev. Lett. **92**, 052302 (2004).
 [30] Z.W. Lin and C.M. Ko, Phys. Rev. Lett. **89**, 202302 (2002).
 [31] D. Molnar and S.A. Voloshin, Phys. Rev. Lett. **91**, 092301 (2003).

- (2003); R.J. Fries *et al.*, *ibid.* **90**, 202303 (2003).
- [32] R.C. Hwa and C.B. Yang, Phys. Rev. C **70**, 024905 (2004).
- [33] V. Greco *et al.*, Phys. Rev. Lett. **90**, 202302 (2003).
- [34] J. Adams *et al.*, Phys. Rev. Lett. **91**, 172302 (2003).
- [35] X.N. Wang, Phys. Rev. C **61**, 064910 (2000); Phys. Lett. B **565**, 116 (2003).
- [36] Y. Zhang *et al.*, Phys. Rev. C **65**, 034903 (2002).
- [37] B.Z. Kopeliovich *et al.*, Phys. Rev. Lett. **88**, 232303 (2002).
- [38] I. Vitev, Phys. Lett. B **562**, 36 (2003).